REDUCING CO_2 EMISSIONS OF CONCRETE SLAB CONSTRUCTIONS WITH THE PRIMECOMPOSITE SLAB SYSTEM

Xavier DESTRÉE
Structural Engineer, Consultant, La Hulpe, Belgium

Brad J. PEASE, Ph.D.
Concrete and Structural Engineer, SIA Primekss, Riga, Latvia

ABSTRACT:
PrimeComposite, a steel fiber reinforced concrete (SFRC) containing proprietary additives to control hygral shrinkage, provides significant reductions in CO_2 emissions per square meter and improved performance over traditional slab on grade systems. This paper describes the development of the PrimeComposite system including the structural design approach, which is based upon full-scale mechanical testing results presented here. A typical PrimeComposite slabs on grade is 10 cm thick with single-casting (jointless) areas of up to 6500 m^2. At this thickness, rack system loads of 140 kN (back-to-back leg loads) are safely supported.
Keywords: steel fiber, shrinkage, jointless slabs, durability, carbon footprint

1. INTRODUCTION

The concrete construction industry depends on environmentally demanding processes, such as mass consumption of energy, raw materials, and transit, and contributes significantly to global carbon dioxide (CO_2) emissions. Globally, Portland cement production emitted 932 million metric tons of CO_2 ($MtCO_2$) in 2002, approximately 7% of all stationary CO_2 sources [1,2]. Typical emission rates between 1995 and 2005 varied from 0.6 to 1.0 kg of CO_2 per kg of Portland cement [3]. While alternatives to Portland cement exist, such as blended cements [4] or low CO_2-emitting cements [5], demand for Portland cement continues to increase [3].

Transport of ready-mix concrete is a secondary, yet significant, source of CO_2 emissions as illustrated in a survey of 99 ready-mix companies located throughout the US in 2006 [6]. The survey, comprising 17,080 concrete trucks that traveled an annual average of 28,760 km per truck (>491 million km total), determined the average fuel economy was 1.52 km/L. Therefore, approximately 324 million liters of diesel were consumed. According to [7], combustion of diesel fuel emits approximately 2.66 kg CO_2/L diesel, resulting in 0.86 $MtCO_2$ emissions due to concrete transport from the 99 companies involved. Clearly worldwide annual emissions from concrete transport are significant.

While the CO_2 emission rates associated with concrete production are far below other common building materials (e.g., steel [5]), significant reductions in the carbon footprint of the industry are possible through the efficient and thoughtful use of Portland cement. One such development, the PrimeComposite concrete slab system [8], seeks to reduce required concrete slab thickness (and corresponding CO_2 emissions), while improving performance and durability compared to traditional slab systems. Thickness reductions are provided using a two-pronged approach: 1) Replacement of all steel reinforcing bars with steel fibers for required tensile and flexural load capacities, and 2) Control of concrete shrinkage with proprietary admixtures. Performance and durability improvements are provided by eliminating the need for saw-cut joints and reducing the number of construction (day) joints. The aim of this paper is to detail the performance improvements and CO_2 emission reductions provided by PrimeComposite slab systems compared to traditional concrete slab systems (welded wire mesh reinforced with saw-cut joints and SFRC without saw-cut joints).

2. DEVELOPMENT OF THE PRIMECOMPOSITE CONCRETE SLAB SYSTEM

Concrete floor slabs (slabs-on-grade and slabs-on-piles) are an essential, yet often overlooked, component in the function and operations of nearly all buildings. Concrete for large industrial, warehouse, retail, etc. spaces face a multitude of potential problems including cracking, curling, extensive opening of construction (day) joints, damage at saw-cut joints, among others. Shrinkage is however the central mechanism behind nearly all other issues. Shrinkage induces cracking, necessitating the inclusion of joints in an attempt to localize and control cracking, and causes slab length reductions that lead to potentially significant openings of construction (day) joints. Figure 1(a) illustrates a typical construction (day) joint opening in a SFRC slab-on-grade without saw-cut joints. Saw-cut joints, which offer only a limited level of cracking control [9], may reach kilometers in length for a single building as joint spacing of 3 meters is common [10]. Problems are

(a)

(b)

Fig 1 (a) Opening and damage at construction joint, coin similar in size to US quarter, and (b) damage at saw-cut joint.

further compounded as the optimal window of time-of-saw-cutting is finite and a function of mixture proportioning and ambient conditions [11]. Saw-cutting too early results in raveling of the concrete surface, while cutting too late may result in uncontrolled cracking [11]. Finally, saw-cut joints allow curling to take place [10] and introduce a point of weakness where damage localizes and requires repair, as shown in Figure 1(b). Saw-cut joint damages commonly occur due to uneven levels of neighboring slabs leading to forklift wheel impact and/or uplift of the concrete away from the soil support system below the slab.

PrimeComposite improves upon ordinary concrete by enhancing the tensile and flexural behavior and by controlling hygral (autogenous and drying) shrinkage, allowing for jointless slabs with thickness reductions up to and exceeding one half the thicknesses of other slab systems. Mechanical property improvements are realized through the controlled addition of steel fibers, while shrinkage control is accomplished by both careful mixture design and the addition of proprietary concrete additives, PrimeDC and PrimeFlow. Steel fibers, PrimeDC, and PrimeFlow are added to a simple concrete, provided by a ready-mix producer, using specialized equipment on the jobsite. Additional details on the development of PrimeComposite and the contributions of the various components are provided in the following sections.

2.1 Steel Fiber Reinforced Concrete

Steel fiber reinforced concrete (SFRC) has been used for over 30 years to reinforce concrete slabs on grade and to limit the required number of shrinkage joints in concrete floors [12,13]. Based on experience using SFRC, typically a continuous field size of up to 1500 m^2 are obtainable with construction (day) joints at a maximum spacing of 40 meters [14]. Concrete for this application typically consists of a C30/37 (30 MPa cylinder strength) strength class with water-to-cement ratio (w/c) below 0.50, and a maximized aggregate content to limit drying shrinkage. Reinforcement is provided by a moderate dosage rate, typically ≥30 kg/m^3, of type I (cold-drawn) steel fibers [15]. Higher dosage rates are also used depending on fiber shape and dimension, service loading, and subgrade bearing capacity.

As discussed in greater detail in Section 3.1 below, full-scale tests simulating SFRC ground-supported slabs exhibit a ductile flexural response with rotations concentrated along yield lines. Additional full-scale experiments presented in literature indicate yield line theory (i.e., flexure) controls design of both pile-supported [14] and elevated [16-18] slabs. Testing of a 20 cm thick elevated slab with 6 meter column spacing and 100 kg/m^3 dosage rate of hooked-end steel fibers indicate between 5 and 7 times the first crack loading is required to cause failure [16]. Under typical loading conditions, punching failure around column or pile heads does not occur due to limited flexural capacity of SFRC [16-18].

Typically SFRC is cast over two layers of plastic sheet to minimize frictional restraint between the subgrade and the shrinking concrete. Steel fibers are highly effective at controlling cracks [19], therefore these slabs typically exhibit minimal cracking. Further, steel fibers offer a reliable control of curling at construction joints and edges are kept at an affordable level and do not affect significantly the serviceability and the durability of the slab. However as shown in Fig 1(a), joint openings in excess of 1 cm are common. Therefore, as discussed in the following section, PrimeComposite includes proprietary additives to control shrinkage and further improve concrete performance.

2.2 Control of Shrinkage

As discussed above, concrete shrinkage critically affects the performance of all slabs. Restrained shrinkage results in random cracking of the slab, while unrestrained shrinkage causes substantial joint openings. Differential shrinkage caused approximately 8 mm of curling at joints and edges after only 50 days with 'optimal' concrete for slab-on-grade applications [10]. In the authors' experience, up to 15 mm of curling has been observed with additional time.

The addition of PrimeDC, a cementitious additive, and PrimeFlow, a liquid admixture, to SFRC controls a lifetime of concrete shrinkage, as shown in Fig 2.

The main advantage of the zero-shrinkage concept is to protect the slab from random cracking since it cancels the adverse effect of the drying shrinkage: crackfree slabs become feasible and thanks to the steel fiber reinforcing, the tensile strength of the slab concrete becomes a viable property that the designer can rely on.

Also the cancellation of the curling along the edges, makes the slab in full and permanent contact to the grade so that negative moment cracking along the joints and edges is no longer a critical loading case to consider anymore.

Construction joints that are needed to separate two consecutive pours remain closed in usual temperature conditions inside a building, so that the load transfer from one slab to the next is total.

As the drying shrinkage is cancelled, it is possible to tie the construction joints without any adverse effect like wild random cracking.

The user sees that type of floor as being like infinite so that they forklift trucks enjoy completely smooth ride without bumps at each joint.

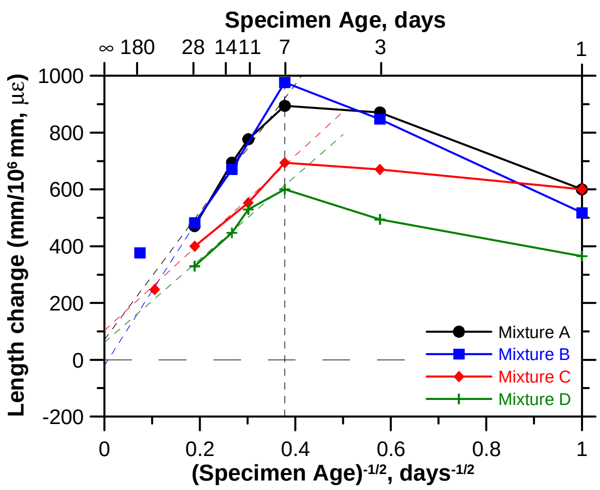

Fig. 2 Zero shrinkage concrete deformations in function of age in days to infinite time.

A typical permanent compression stress of up to 2.0 MPa takes place in the slab section when the slab is subjected to a movement restraint by the friction from the granular base. In Fig 2, it is shown that a permanent 10-15 με in compression is being reached at infinite age.

3. STRUCTURAL DESIGN

3.1 Full-Scale Structural Testing

A full scale test of a zero shrinkage slab subjected to a point loading has been organized at the University of Vaasa in Finland as shown in Fig 3.

The aim was to measure the deformation of the slab, including sagging underneath the point loading application and hogging at some distance away, the first cracking load and the ultimate loading intensity as well. The test slab had the following characteristics:

Square slab of 4 m x 4 m size and of 100 mm thickness, resting on a base of 100 mm thickness of EPS 200 polystyrene with E =10 MPa and 0.09 MPa long term compressive strength at 1% deformation.

A portal frame was used to impose by mean of a hydraulic jack, a center point loading intensity with a contact disk plate of 125 mm diameter.

The concrete compressive strength was of 32 MPa and the reinforcing of the slab was of 35 kg/m³ of randomly distributed hooked-end steel fiber of 0.75 mm diameter, 50 mm length, and 1100 MPa tensile strength.

The insulation layer was installed on top of a concrete strong floor and the resulting K_w bearing coefficient of Westergaard was also measured with the 760 mm round plate diameter: K_w = 30 MPa/m.

The radius of rigidity of the slab of 100 mm thickness L_r is calculated according to the theory of Westergaard, according to Eq. 1:

$$L_r = \sqrt[4]{\left(\frac{Eh^3}{12(1-\nu^2)} K_w\right)} \qquad \text{Eq. 1}$$

Fig. 3 Test set-up of the center point loading.

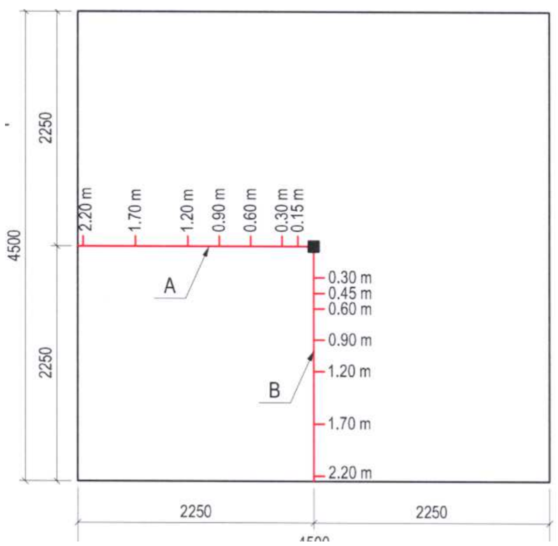

Fig. 4 Aerial view of the test set-up with measurement locations.

where h = 100 mm, thickness of slab.

E = 30000 MPa, Modulus of elasticity of concrete.

υ = 0, coefficient of Poisson of EPS 200.

K_w = 0.03 N/mm³, coefficient of Westergaard.

so that L_r =537mm.

The deflections of the slab are recorded along x and y axis at 0.15, 0.30, 0.60, 0.90, 2.20 m distance from the center point.

As shown in Fig 5, when the centre point loading intensity increases from 10 kN to 213 kN, the zero deflexion abscissa is situated between 500 mm and 600 mm distance to the slab centre. This confirms the calculation of Lr = 537 mm the radius of rigidity of the slab.

The ultimate loading intensity at collapse of the slab was recorded at 270 kN point loading intensity.

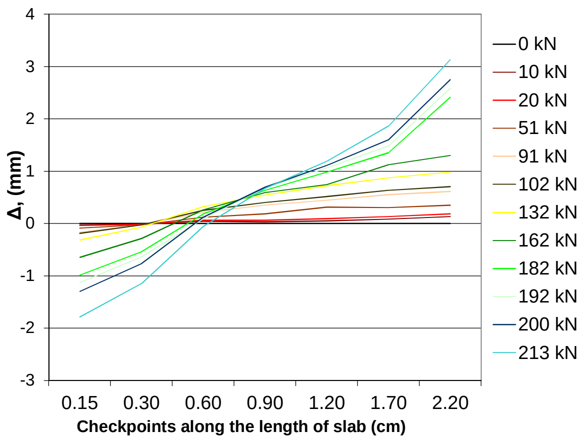

Fig. 5 Deflections recorded from 0.3 m distance to 2.20 m distance.

3.2 Design Procedure

The design of a center point loading case is finalized by assuming a plastic slab showing yield lines in a fan pattern of the positive moment and together with a circular yield line. The external moment equilibrium takes into account the point loading intensity and the elastic reaction of the EPS200. Permanent deformations of the EPS200 insulation layer are not accepted and not acceptable.

The typical theory and equation of the equilibrium of the moments has been developed and written by F.Van Cauwelaert [20], as shown in Eq 2:

$$m + m' = \frac{P}{2\pi}\cdot\left(1-\frac{8}{9}\cdot\sqrt[3]{\frac{\pi}{32}}\cdot\sqrt[6]{\frac{kc^4}{EI}}\right)-\frac{P}{144}\cdot\sqrt{\frac{k}{EI}}\cdot\sqrt[3]{\frac{1024EIc^2}{\pi^2 k}} \qquad \text{Eq. 2}$$

Where:

m and m' are the positive and negative resisting yield moment of the steel fiber reinforced concrete.

m = - m' = 11.6 kNm/m

k is the reaction coefficient of Westergaard.

E the modulus of elasticity of the concrete

I: the moment of inertia of the slab

c: the radius of the point loading

The equation of Van Cauwelaert in this case gives an ultimate loading intensity of P_{ult} = 172 kN and a maximum service point loading intensity of 77 kN.

The deflection is still smaller than 0.5 mm as can be seen on Fig 5 regarding the line in yellow, thus less than 0.5% of the thickness of the EPS200 insulation. Such a deformation of 0.5% is ¼ of the 2% limit of deformation of the EPS 200 insulation and thus results in a pressure of ¼ of the 0.09 MPa limit pressure or 0.0225 MPa.

It is verified also that 77000 N/πL_r^2 = 0.085 MPa, the average pressure underneath the slab under the center point loading, is almost the limit pressure of 0.09 MPa under long term service condition. We conclude that the plastic design of the slab onto an elastic base leads to a quite realistic and safe estimate of the maximum permissible center point loading intensity in service. Indeed at 77 kN point loading intensity, the global safety to rupture is of 270kN / 77kN = 3.50.

The section of slab at the plastic stage undergoes a nonlinear distribution of stresses across the section. Indeed, we assume a constant tensile plastic strength f_{tu} distributed on 90% of the section of the slab as the 10% remaining is uncracked and under compression. Hence we can write [20]:

$$m = 0.45 f_{tu} h^2 \qquad \text{Eq. 3}$$

and also:

$$f_{tu} = \frac{11600}{0.45} \times 100^2 = 2.57\ N/mm^2 \qquad \text{Eq. 4}$$

Such a value is derived from a full scale test and as such cannot be deducted from standard prismatic specimen in flexion of EN14651 or other similar standards.

Indeed, the experimental calculation here includes an application factor influenced by the size of the slab and by the nature of the zero shrinkage concrete.

As these observations are derived from a full scale testing, the values calculated experimentally are indeed characteristic values.

When the K_w of Westergaard is increased from 0.03 N/mm³ to 0.08 N/mm³ and that all other parameter are kept constant, the moment and the maximum permissible point loading intensity are increased by almost 50%.

Hence a zero-shrinkage fiber reinforced concrete slab of 100 mm thickness on top of a base showing K_w = 0.08 N/mm³, becomes suitable in case of point loading intensities of up to 115 kN. When compared to a traditional slabs, 60 mm to 80 mm thickness of concrete are saved.

As shown in Fig. 6, a diagram summarizes the thickness needed in function of the statical point loading intensity in case of a steel fibre reinforced zero-shrinkage concrete slab. The diagram has been calculated for K_w = 0.08 N/mm³ and mention the leg load intensity of a back-to-back case of leg loadings.

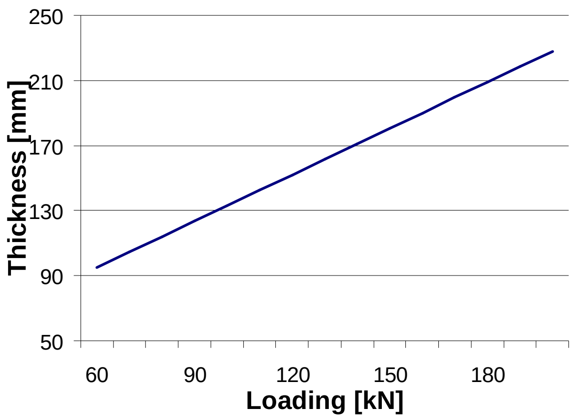

Fig. 6 Design diagram: Thickness vs. Point loading Intensity of a back to back leg case.

3.3 Case Studies

Since the year 2007, approximately 1.1 million m² of SFRC zero-shrinkage slabs have been successfully completed to the full satisfaction of the customer and the end-user.

With a normal shrinkage concrete slab as described in the introduction, a minimum thickness of 150 mm should have been is needed as outlined in [17].

When using a zero-shrinkage slab, as full continuity is obtained across the construction joints, the only loading case to verify is that of the centre point loading. The edge and corner cases of point loading do not exist anymore. Against the perimeter wall, there is indeed no traffic and the shelves are only loaded on one side thus at the half of the full intensity.

Between two adjacent buildings, the very edge of each slab is subjected to the full traffic intensity: a local thickening of the slab at 30 degree angle and without stepping, is a common solution.

Typical reference projects:

- Norwegian Post Office warehouse, 42000 m², 110 mm, 2×70 kN point loading
- Unil Logistic Center (Norway), 120 mm, 2 x 75 kN point loading
- MAP high storage (Sweden), 4000 m², 150 mm, 2 x 112 kN
- John Deere, Marsta (Sweden), 7000 m², 100 mm, 2 x 50 kN
- Antalys, Marsta (Sweden), 15000 m², 120 mm
- Prologis, Jonkoping (Sweden), 15000 m², 100 mm
- Asko, Molde (Norway), 4700m², 100 mm
- Inex (Finland), 20000 m², 120 mm
- Sipoo Lemminkainen (Finland), 48000 m²
- Vlantana Freezer, Klaipeda (Lituania), 4700m²

4. REDUCTIONS IN CO_2 EMISSIONS

Table 1 provides statistics on the average thicknesses (weighted by area of individual slabs) and total areas of PrimeComposite and other concrete slab on grade systems cast between January and August 2012 by SIA Primekss. Other slab on grade systems included simple welded-wire mesh reinforced slabs with saw-cut joint and traditional steel fiber reinforced jointless floors. PrimeComposite slabs had an average thickness of 11.8 cm, including 10,800 m² PrimeComposite slab with 18 cm thickness designed for point loads of 200 kN. Alternative slab systems were approximately 46% thicker with a weighted average thickness of 17.2 cm. Nearly twice the area of PrimeComposite slabs were cast compared to other slab solutions with only approximately 31% additional concrete volume. If PrimeComposite slabs were replaced with other systems (i.e., using the average thickness of other slab solutions) an additional 20,600 m³ of concrete would be needed or 43,170 m³ of concrete in total.

CO_2-emissions related to the production of Portland cement occur at rates between 0.6 and 1.0 tons CO_2/ton cement, with the weighted average in 2005 being 0.83 tons CO_2/ton cement [3]. In the following calculations, CO_2-emissions related to PrimeDC production are assumed to be identical to Portland cement, which is

Table 1 Statistics on PrimeComposite and other slab on grade systems according to internal documentation.

Slab type	Avg. thickness	Area cast	Concrete volume
	cm	m^2	m^3
PrimeComposite	11.8	250,984	29,616
Other	17.2	131,220	22,570

likely a conservative assumption as production of PrimeDC requires a lower kiln temperature and less calcium carbonate than Portland cement.

On average, the total cementitious content of PrimeComposite (i.e., Portland cement and PrimeDC), is nearly identical to other slab systems. Current production totals presented in Table 1 result in cement-related CO_2-emission rates of 28.9 kg CO_2/m^2 for PrimeComposite slabs and 42.1 kg CO_2/m^2 for saw-cut and traditional jointless floors. This accounts for more than 31% reduction in CO_2 per area of slab placed.

According to internal documentation a total of approximately 1,100,000 m^2 of PrimeComposite slabs on grade have been placed to date. Based on the thicknesses shown in Table 1, PrimeComposite (compared to other slab systems) has saved of approximately 15,900 tons of Portland cement and reduced Primekss' carbon footprint of approximately 12,585 tons of CO_2.

Comparisons presented to this point are focused on the quantities of cement used. However, secondary sources of CO_2-emission reduction are likely considerable, for example reduced transportation and steel demand.

From January to August 2012, PrimeComposite slabs resulted in a 20,600 m^3 reduction in required concrete volume. Delivery of this volume of concrete would involve between 2060 to 3430 truckloads, depending on drum volume. As discussed in the introduction section, average fuel economy for concrete trucks was 1.52 km/L in 2006 [6], and diesel fuel combustion emits 2.66 kg CO_2/L diesel [7]. Assuming a one-way delivery distance of 10 km, approximately 166-277 additional tons of CO_2 would have been emitted during an 8 month period. Additionally, up to 15,450 m^3 of aggregate and CO_2 emissions related to production and transportation were saved as typically 75% of the volume of concrete consists of aggregate.

A further reduction of the carbon footprint of PrimeComposite slabs is provided by the minimization of reinforcing steel. Traditional jointless slabs require a minimum reinforcement ratio of 0.5% in both directions [21]. Assuming the average thickness of these slabs in Table 1, a total of 13.4 kg of reinforcing steel is required per square meter of slab ($A_s = 0.5\% \times 172 \text{ mm} \times 1000 \text{ mm} \times 2 = 1720 \text{ mm}^2/\text{m}$, $1720 \text{ mm}^2/\text{m} \times 7800 \text{ kg/m}^3 = 13.4 \text{ kg/m}^2$ slab). The steel fiber dosage from the full-scale results in section 3, 35 kg/m^3 and the average thickness of PrimeComposite slabs, 11.8 cm yields a steel consumption of only 4.1 kg steel per square meter of slab. As steel production typically emits in excess of 1 kg CO_2 per kg steel [22,5], a further reduction of no less than 9.3 kg CO_2/m^2 of slab is realized.

Considering the reduced volumetric demand for cement and steel of PrimeComposite slabs, CO_2 emissions are reduced by 22.5 kg CO_2 or 40.5% per square meter of of slab.

5. CONCLUSIONS

Results presented in the paper conclude the following:

- Using the proprietary additives PrimeDC and PrimeFlow control shrinkage of concrete, allowing for jointless slabs sections with areas up to 6500 m^2. Shrinkage cracking, curling, and joint opening are significantly reduced or eliminated.
- Full-scale testing of PrimeComposite slabs indicated a 100 mm thick slab, with sufficient quality subgrade, supports point loads up to 115 kN.
- CO_2 emissions are reduced by no less than 40.5% by replacing traditional concrete slab systems with PrimeComposite.

REFERENCES

1. International Energy Agency (IEA), "Building the Cost Curves for CO2 Storage, Part 1: Sources of CO2," IEA Publications, PH4/9, 2002, 48 pp.
2. Metz, B., Davidson, O., de Coninck, H., Loos, M., Meyer, L., "Carbon Dioxide Capture and Storage," Intergovernmental Panel on Climate Change (IPCC), 2005, 431 pp.
3. International Energy Agency (IEA), "Tracking industrial energy efficiency and CO_2 emissions," IEA Publications, 2007, 321 pp.
4. Blair, B., "Cementitious blends and their impact on sustainable construction," ACI Special Publication 269, 2009, pp. 27-36.
5. Gartner, E., "Industrially interesting approaches to "low-CO_2" cements," Cement and Concrete Research, Vol. 34, 2004, pp. 1489-1498.
6. Carew, J., Green, T., Benjamin, A., Moore, P., Mullings, G., "2007 National Ready Mixed Concrete Association Fleet Benchmarking and Costs Survey," Concrete In Focus, Vol. 6, 2007, pp. 11-30.
7. United States Environmental Protection Agency (EPA), "Average Carbon Dioxide Emissions Resulting from Gasoline and Diesel Fuel," 2005, 3 pp.
8. Ošlejs, J., Kravalis, K., "Composite concrete for floor slabs and rafts," US Patent application US2012/0021206 A1, 2012, 6 pp.
9. Gu, X., Song, X., Lin, F., Li, C., Jin, X., "Cracking behaviour of cast in situ reinforced concrete slabs with control joints," Construction and Building

Materials, Vol. 25, No. 3, 2011, pp. 1398-1406.
10. Vruno, D., Ramerth, M., "Optimum Slab-on-Ground Concrete," Concrete International, Vol. 34, No. 7, 2012, pp. 40-45.
11. Their, T., "Examining the time and depth of saw-cutting guidelines for concrete pavements," Master's thesis, Purdue University, West Lafayette, IN, USA, 2005, pp. 170.
12. Destrée, X., Lazzari, A., "Industrial Floor and Construction Method," US Patent 4,640,648, 1984, 3 pp.
13. Destrée, X., Lazzari, A., "Procede de fabrication d'un sol industriel," European patent 0137024, 1984, pp. 4.
14. Oslejs, J., "New frontiers of steel fiber-reinforced concrete," Concrete International, Vol. 30, 2008, pp. 45-50.
15. ASTM A820, "Standard Specification for Steel Fibers for Fiber-Reinforced Concrete," ASTM International, West Conshohocken, PA, 2011, DOI: 10.1520/A0820_A0820M-11, www.astm.org.
16. Destrée, X., "Steel-fiber-only reinforced concrete in free suspended elevated slabs," Concrete Engineering International, Spring 2009, pp. 47-49.
17. Destrée, X. "Structural application of steel fibre as only reinforcing in free suspended elevated slabs" RILEM proceedings PRO39, BEFIB2004, pp1073-1082.
18. Michels, J., Waldmann, D., Maas, S., Zürbes, A., "Steel fibers as only reinforcement for flat slab construction – Experimental investigation and design," Construction and Building Materials, Vol. 26, No. 1, 2012, pp. 145-155.
19. Pease, B., Shah, H., Hossain, A., Weiss, J., "Restrained shrinkage behavior of mixtures containing shrinkage reducing admixtures and steel fibers," Proceedings of the International Conference on Advances in Concrete Composites and Structures, Chennai, India, 2005.
20. Van Cauwelaert, F., "Evolution dans le dimensionnement rationnel des revêtements eb béton et des sols industriels" Bouwkroniek, Oct. 1996, pp. 24-34.
21. Eurocode 2: Design of Concrete Structures CEN - European Committee for Standardization, 2003
22. L. Price, E. Worrell, D. Phylipsen, "Energy use and carbon dioxide emissions in energy-intensive industries in key developing countries," Proceedings of the 1999 Earth Technologies Forum, Washington, DC, Sept. 27– 29, 1999.